Site-Specific Geometric and Electronic Relaxations at Organic-Metal Interfaces

H. Yamane,[1] A. Gerlach,[2] S. Duhm,[3,4] Y. Tanaka,[5] T. Hosokai,[2] Y. Y. Mi,[6] J. Zegenhagen,[6] N. Koch,[3] K. Seki,[5] and F. Schreiber[2]

[1]*Institute for Molecular Science, Okazaki 444-8585, Japan*
[2]*Institut für Angewandte Physik, Universität Tübingen, D-72076 Tübingen, Germany*
[3]*Institut für Physik, Humboldt-Universität zu Berlin, D-12489 Berlin, Germany*
[4]*Graduate School of Advanced Integration Science, Chiba University, Chiba 263-8522, Japan*
[5]*Department of Chemistry, Graduate School of Science, Nagoya University, Nagoya 464-8602, Japan*
[6]*European Synchrotron Radiation Facility, 38043 Grenoble Cedex 9, France*

(Received 2 April 2010; published 23 July 2010)

The correlation between the geometric and electronic structures of Zn-phthalocyanine (ZnPc) and F_{16}ZnPc on Cu(111) were studied by x-ray standing wave and angle-resolved photoemission spectroscopy. We found evidence for a distortion of the planar molecules upon adsorption, with the central Zn atom in the molecule protruding towards the substrate. This modifies the energy levels of both the molecule and the substrate, which appear as interface states. The site-specific geometric and electronic relaxations are an important effect for organic-metal interface energetics.

DOI: 10.1103/PhysRevLett.105.046103 PACS numbers: 68.43.−h, 73.20.−r, 79.60.Dp, 81.05.Fb

The rapid recent progress in organic semiconductor devices is expected to pave the way for next-generation nanoelectronics. Organic-metal (O-M) interfaces are essential for device performance, and they also represent a formidable testing ground for complex fundamental effects related to (partially) delocalized electron and hole states and their transfer between molecules and metals. In this context, the energy level alignment near the Fermi energy (E_F), such as the highest-occupied and lowest-unoccupied molecular orbitals (HOMO and LUMO), is crucial. However, O-M interface energetics are rather complicated because of the existence of interface dipoles (ID) and interface states (IS) [1,2], which are either intrinsic due to the interface formation or extrinsic due to the presence of impurities and/or defects. These effects are not well understood on a fundamental level, yet several possible factors of ID and IS, such as O-M charge transfer (CT) [3], have been demonstrated for the control of O-M interface energetics. For the further elucidation towards the intentional control of O-M interfaces, a more pertinent approach would be to use a well-characterized system for quantitative complementary measurements.

The x-ray standing wave (XSW) technique is a high-precision method to probe site-specific adsorption heights between adsorbate atoms and substrate surfaces [4–12]. The O-M distance is an important factor in the formation of ID [13] and IS [14]. Therefore, the XSW technique has recently been applied to large π-conjugated systems. In this Letter, we focus on the important question of how the adsorbate configuration affects the interfacial electronic structure. In order to explore this question, we applied the combination of XSW and angle-resolved photoemission spectroscopy (ARPES), which enables the comprehensive understanding of the correlation between geometric and electronic structures, to Zn-phthalocyanine (ZnPc) on a Cu(111) surface. Since organometallic compounds, such as Pc's, contacted with metals show various electronic and magnetic properties, the present study can be regarded as an archetypal model wherein the influence of a metal atom in the molecule on the geometric and electronic structures can be studied. From the XSW data, we infer the ZnPc-Cu(111) bonding configuration, and find significant molecular distortion with the central Zn atom in the molecule protruding towards the substrate. The ARPES data reveal the formation of two IS derived from the substrate surface modification and the molecular distortion. Furthermore, these geometric and electronic phenomena can be substantially modified by fluorination of the molecule (F_{16}ZnPc). Based on these results, we address the importance of site-specific geometric and electronic relaxations at O-M interfaces.

The experiments were performed at the synchrotron radiation facilities ESRF ID32 for XSW and UVSOR BL8B2 for ARPES. The experimental setup and data analysis procedures are described in Ref. [6] for XSW and Ref. [15] for ARPES. For XSW, we used the (111) Bragg reflection in normal incidence geometry. All XSW and ARPES data were measured at 300 K. The clean Cu(111) was obtained by repeated cycles of Ar^+ sputtering and annealing at 750 K, as confirmed by core-level peaks in XSW and by the surface state and the work function (Φ) in ARPES. Purified ZnPc and F_{16}ZnPc was evaporated onto the clean Cu(111) at a rate of 1 Å/min. The monolayer (ML) coverage was determined from the core-level peaks in XSW and the Φ change in ARPES.

First, we discuss the site-specific O-M interaction at ZnPc/Cu(111), which was examined by XSW (Fig. 1). By measuring the photoelectron yield of Zn $2p_{3/2}$, N $1s$,

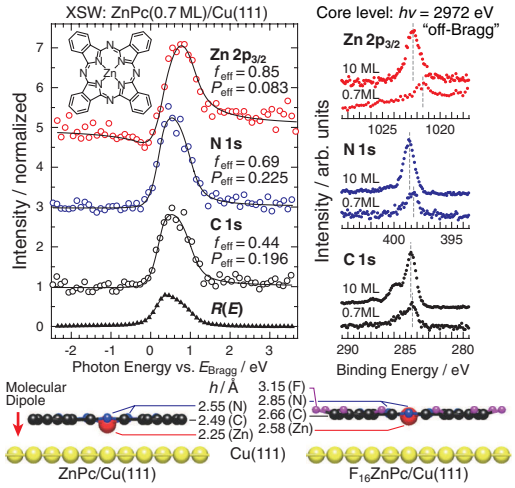

FIG. 1 (color online). Zn $2p_{3/2}$, N 1s, and C 1s photoelectron and x-ray reflectivity $[R(E)]$ profiles as a function of $h\nu$ relative to the Bragg energy for ZnPc(0.7 ML)/Cu(111). The best fits to the experimental data (○) yield the coherent fractions (f_{eff}) and coherent positions (P_{eff}) used to determine the bonding configuration, shown at the bottom.

and C 1s for the photon energy ($h\nu$) around the substrate Bragg condition (2.97 keV), characteristic XSW signals are obtained at 0.7 ML. Compared to the C and N data sets, the Zn atom shows a notably different signal. Analysis of the XSW data gives the coherent fraction (f_{eff}) and coherent position (P_{eff}) for different atoms, which are directly related to the ordering and structure of adsorbates [4]. The relatively large f_{eff} for N and Zn indicates that the film is well ordered with a flat-lying orientation. The smaller f_{eff} found for C indicates slightly different adsorption heights of the inequivalent C sites that cannot be distinguished in this experiment. From P_{eff}, we then obtain the average O-M adsorption height (h) with respect to the substrate lattice: $h_{\mathrm{C}} = 2.49 \pm 0.03$ Å for the C atoms, $h_{\mathrm{N}} = 2.55 \pm 0.02$ Å for the N atoms, and $h_{\mathrm{Zn}} = 2.25 \pm 0.05$ Å for the Zn atom. Hence, the planar ZnPc is significantly distorted and exhibits a nonplanar conformation on Cu(111), with the Zn atom protruding significantly towards the substrate compared to the Pc ligand. Moreover, h_{C} of 2.49 Å for ZnPc/Cu(111) is relatively small compared to other organic molecules on Cu(111); F_{16}CuPc (2.61 Å) [6], 3, 4, 9, 10-perylene tetracarboxylic dianhydride PTCDA (2.66 Å) [8], and perfluoropentacene (2.98 Å) [11]. As discussed for the strongly chemisorbed pentacene (2.34 Å) [11], a small h_{C} causes a large Pauli repulsion which affects the energy level alignment. Note, however, that additional O-M charge rearrangements occur for chemisorbed molecules. Furthermore, the molecular distortion of ZnPc modifies MOs related to a Zn-N bond and results in a molecular dipole directed towards the substrate.

The molecular distortion and small h's of ZnPc on Cu(111) are significantly changed by fluorination of the molecule. Compared to ZnPc, the XSW data for F_{16}ZnPc/Cu(111) give consistently larger P_{eff} [16], which result in $h_{\mathrm{Zn}} = 2.58 \pm 0.05$ Å, $h_{\mathrm{C}} = 2.66 \pm 0.10$ Å, $h_{\mathrm{N}} = 2.85 \pm 0.02$ Å, and $h_{\mathrm{F}} = 3.15 \pm 0.09$ Å (Fig. 1). The larger h's of all atoms in F_{16}ZnPc obviously correlate with the comparably small protrusion of the Zn atom.

On the basis of the bonding configuration, we now discuss the interfacial electronic structure. Figure 2(a) shows the emission angle (θ) dependent ARPES data for ZnPc/Cu(111) as a function of the coverage measured with an energy resolution of 0.1 eV at 300 K and an angular resolution of 0.8°. For the clean Cu(111) at $\theta = 0°$, the Shockley surface state (S) peaks at a binding energy (E_b) of 0.39 eV. Remarkably, the Shockley state is not fully quenched even for 1 ML ZnPc, but shows a continuous peak shift at 0–1 ML ($S \rightarrow S_1$). This peak S_1 disappears by further deposition while peak H_1 evolves and shifts to a higher E_b. At $\theta = 50°$, peak H_1 becomes more intense, and an interface-specific peak X_1, which does not shift at 0–1 ML, appears near E_F with a different line shape compared to peak S_1. This evidence is clearly seen in the ARPES intensity map. From these results, we conclude that peak H_1 is derived from the HOMO while peaks S_1 and X_1 are IS with mutually different origin. Such peaks are also observed for F_{16}ZnPc/Cu(111) with slightly different characteristics [Fig. 2(b)], (i) low-E_b shift in peak H_2 with increasing coverage, (ii) E_b position of peak S_2, and (iii) relatively weak peak X_2. These IS near E_F are crucial for the interface energetic and will significantly influence charge transport across such an interface.

In order to analyze the adsorption-induced peaks, we focus on the detailed θ dependence of ARPES for 1 ML ZnPc [Fig. 2(c)]. The remanent Shockley state S_1 shows a continuous peak shift at $\theta = 0° - \pm 6°$, and disappears at $\theta \sim \pm 7°$. The energy-vs-momentum $E(\boldsymbol{k}_{\parallel})$ relation of peak S_1 shows a free-electron-like dispersion as for the substrate. This implies that peak S_1 is derived from the Shockley state; however, the E_b position and the effective mass (m^*) undergo characteristic changes compared to the clean Cu(111). At $\theta = 15°$–$58°$, two other nondispersive peaks appear at $E_b = 1.44$ eV (H_1) and 0.25 eV (X_1) with a different intensity distribution $[I(\theta)]$ as shown in the intensity map and its polar plot. Note that the PES-intensity angular distribution reflects the spatial distribution of MOs [17,18]. Thus, the observed $I(\theta)$ gives further information on the adsorption-induced peaks as discussed later. Similar trends are also observed for F_{16}ZnPc (not shown).

From the present ARPES data and previous work with inverse photoemission [2,19], we compiled the energy diagram of ZnPc/Cu(111) and F_{16}ZnPc/Cu(111) in Fig. 2(d). Considering the energy difference of the HOMO, LUMO, and E_F with respect to the vacuum level (VL) before the O-M contact, CT from the Cu(111) to the LUMO is not anticipated for both ZnPc and F_{16}ZnPc since the E_F is located in the HOMO-LUMO gap. From this point of view, the strong peak X_1 for ZnPc/Cu(111) is, in particular,

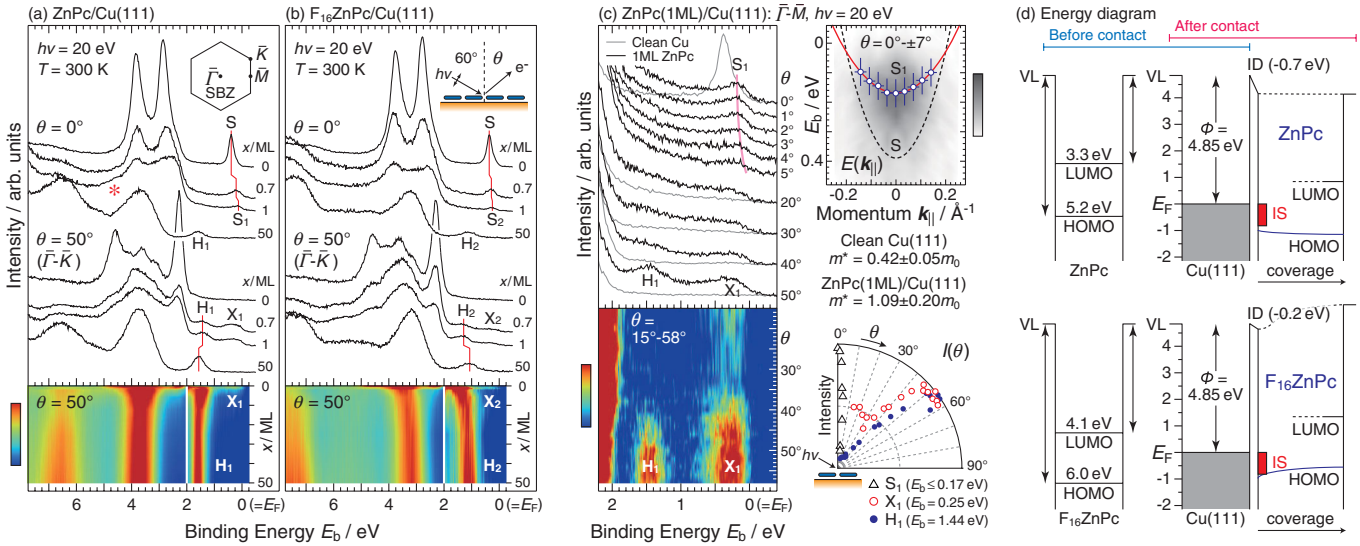

FIG. 2 (color online). Coverage dependence of ARPES and its intensity map for (a) ZnPc and (b) F_{16}ZnPc on Cu(111) measured at $h\nu = 20$ eV. (c) θ dependence of ARPES and its intensity maps of 1 ML ZnPc on Cu(111). (d) Energy diagrams of ZnPc/Cu(111) and F_{16}ZnPc/Cu(111), where the LUMO energy for F_{16}ZnPc is estimated from that for F_{16}CuPc [2].

unexpected. If peak X_1 originates either from the former LUMO as reported for potassium-doped ZnPc [19] or from the level splitting due to orbital hybridization as reported for pentacene/Cu [15], deeper-lying energy levels should be affected as well. These scenarios seem unlikely for the present interfaces since (i) deeper-lying valences do not show a significant shift for 1–5 ML, and (ii) the C 1s and N 1s PES for 0.7 ML are similar to those for 10 ML (see, Fig. 1).

Based on the bonding configuration, the MOs related to the Zn-N bond may play a crucial role for peaks $X_{1,2}$. We examined the electronic structure of an isolated ZnPc molecule as a function of the Zn-N bond length perpendicular to the Pc plane ($\delta_\perp$) by a MO calculation using GAUSSIAN03 [20]. In Fig. 3, it is seen that the calculated spectrum for $\delta_\perp = 0$ Å (optimized geometry) agrees well with the experimental spectrum of the ZnPc thick film. In contrast to the HOMO (H) and LUMO (L), an unoccupied MO derived from Zn 4s (Z) shows a large energy shift with $\delta_\perp$. Most likely, this effect is more pronounced by the substrate, i.e., the site-specific O-M wave function overlap due to the anisotropic spatial distribution of MOs. In the present case, the Zn-N bond changes from covalent to a more ionic character, and thereby, Zn 4s states can be occupied by CT from the substrate at the Zn site, which is supported by the Zn $2p_{3/2}$ photoemission spectra with relatively large shift at 0.7–10 ML in Fig. 1. These site-specific geometric and electronic relaxations may contribute to peaks $X_{1,2}$. Such evidence also appears for deeper-lying valences. In the experimental data at $\theta = 0°$ [Fig. 2(a)], there is an interface-specific shoulder around $E_b = 5$ eV labeled by $*$, wherein the modification of the MOs related to Zn 3d with $\delta_\perp$ exists. This evidence also supports the present scenario with the site-specific O-M interaction.

The site-specific electronic relaxation is also supported by the ARPES intensity. Using the calculated MOs combined with the single-scattering (SS) approximation, which has successfully reproduced the experimental data [17], the simulated $I(\theta)$ of the flat-lying distorted ZnPc is shown at the bottom of Fig. 3. The calculated HOMO (H) and LUMO (L) derived from C 2p and N 2p show the similar

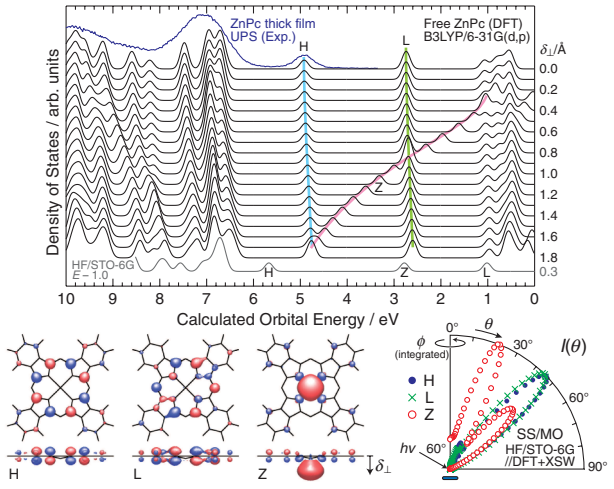

FIG. 3 (color online). Calculated electronic structure of an isolated ZnPc as a function of the Zn-N bond length perpendicular to the Pc plane ($\delta_\perp$), using B3LYP/6-31G(d, p) with Gaussian broadening of 0.2 eV. The MO patterns of H, L, and Z at $\delta_\perp = 0.3$ Å and their PES-intensity θ distribution based on the SS/MO approximation with HF/STO-6G//B3LYP/6-31G (d, p) are shown at the bottom.

$I(\theta)$ pattern with a prominent maximum at $\theta \sim 45°$. The Zn-derived MO (Z) shows a different trend, wherein two maxima appear at $\theta = 22°$ and 46°. Although the perfect agreement between the present experiment (hybrid interface) and the simulation (isolated molecule) is not expected due to the possible site-specific orbital hybridization and delocalization at the interface, the simulated trends can explain the experimental $I(\theta)$ in Fig. 2(c). The θ position for the intensity maxima of the experimental HOMO peak H_1 ($\theta = 55°$) is slightly different from that of the simulated HOMO ($\theta = 46°$), indicating the small orbital modification at the interface. The experimental peak X_1 with two intensity maxima at $\theta = 20°$ and 52° can be ascribed to the Zn-derived MO, which shows two intensity maxima in the simulation. The different relative intensity of peak X_1 and the simulated Zn-derived MO indicates the large orbital modification at the interface due to the protrusion of the Zn atom towards the substrate.

With the above results, the strong peak X_1 for ZnPc on Cu(111) can be ascribed to the Zn-derived IS due to the large molecular distortion and the corresponding electronic equilibration at the interface. Such a distortion-induced IS can be weakened by the larger O-M distance (i.e., smaller molecular distortion) as demonstrated by fluorination of the molecule (F_{16}ZnPc).

The site-specific geometric and electronic relaxations should also affect the Shockley state, which is sensitive to surface modifications. The Shockley state modification upon adsorption of large organic molecules is still under debate due to various physisorptive or chemisorptive bonding scenarios; e.g., PTCDA/Ag(111) shows a large upshift of 0.66 eV [21], whereas pentacene/Cu(110) shows a small downshift of 0.11 eV [22]. In fact, ZnPc/Cu(111) shows a small upshift of 0.22 eV [Fig. 2(c)], even though one might expect a larger upshift because of the strong Pauli repulsion due to the relatively small h_C. Since the observed modification cannot be explained only by the Pauli repulsion, the Shockley state modification for ZnPc/Cu(111) and F_{16}ZnPc/Cu(111) could be dominated by the complex interplay of the O-M interactions, such as the Pauli repulsion and the site-specific CT. Based on the possible origin of the Shockley state modification for ZnPc/Cu(111) and F_{16}ZnPc/Cu(111), we infer that both physical and chemical effects play a crucial role in the stabilization of the electrostatic potential at the interface.

In conclusion, using the combination of XSW and ARPES for ZnPc/Cu(111) and F_{16}ZnPc/Cu(111), we have demonstrated that site-specific O-M interactions and resultant geometric and electronic relaxations yield a comprehensive energetic picture at the O-M interfaces. Among these, the observation of IS due to the change in the Zn-N bond, i.e., distortion-induced IS, is a new, important, and tunable mechanism in O-M interface energetics. We note that the site-specific electronic relaxation should occur not only for other Pc molecules but also other organic molecules when significant modifications of the molecular structure exist at O-M interfaces, such as partial rehybridization of atoms upon adsorption. Moreover, the above scenario is the intramolecular contribution to the electronic structure. Both the intra- and the intermolecular [23] site-specific contributions should affect the total energy relaxation.

The authors like to thank the staff of ESRF and UVSOR for assistance. Financial support by the JSPS, the DFG, and the ESRF is acknowledged.

[1] H. Ishii, K. Sugiyama, E. Ito, and K. Seki, Adv. Mater. **11**, 605 (1999).
[2] J. Hwang, A. Wan, and A. Kahn, Mater. Sci. Eng., R **64**, 1 (2009).
[3] N. Koch, S. Duhm, J. P. Rabe, A. Vollmer, and R. L. Johnson, Phys. Rev. Lett. **95**, 237601 (2005).
[4] J. Zegenhagen, Surf. Sci. Rep. **18**, 202 (1993).
[5] L. Cheng, P. Fenter, M. J. Bedzyk, and N. C. Sturchio, Phys. Rev. Lett. **90**, 255503 (2003).
[6] A. Gerlach *et al.*, Phys. Rev. B **71**, 205425 (2005).
[7] A. Hauschild *et al.*, Phys. Rev. Lett. **94**, 036106 (2005).
[8] A. Gerlach, S. Sellner, F. Schreiber, N. Koch, and J. Zegenhagen, Phys. Rev. B **75**, 045401 (2007).
[9] S. K. M. Henze *et al.*, Surf. Sci. **601**, 1566 (2007).
[10] L. Romaner *et al.*, Phys. Rev. Lett. **99**, 256801 (2007).
[11] N. Koch *et al.*, J. Am. Chem. Soc. **130**, 7300 (2008).
[12] C. Stadler *et al.*, Nature Phys. **5**, 153 (2009).
[13] Y. Morikawa, H. Ishii, and K. Seki, Phys. Rev. B **69**, 041403(R) (2004).
[14] H. Vázquez, Y. J. Dappe, J. Ortega, and F. Flores, J. Chem. Phys. **126**, 144703 (2007), and references therein.
[15] H. Yamane *et al.*, Phys. Rev. B **76**, 165436 (2007).
[16] See supplementary material at http://link.aps.org/supplemental/10.1103/PhysRevLett.105.046103 for extra supporting data.
[17] S. Kera *et al.*, Chem. Phys. **325**, 113 (2006), and references therein.
[18] P. Puschnig *et al.*, Science **326**, 702 (2009).
[19] T. Schwieger, M. Knupfer, W. Gao, and A. Kahn, Appl. Phys. Lett. **83**, 500 (2003).
[20] GAUSSIAN03, D.01, Gaussian, Inc., Wallingford CT, 2004.
[21] C. H. Schwalb *et al.*, Phys. Rev. Lett. **101**, 146801 (2008).
[22] A. Scheybal *et al.*, Phys. Rev. B **79**, 115406 (2009).
[23] S. Soubatch, C. Weiss, R. Temirov, and F. S. Tautz, Phys. Rev. Lett. **102**, 177405 (2009).